

FM MAY 23 1969



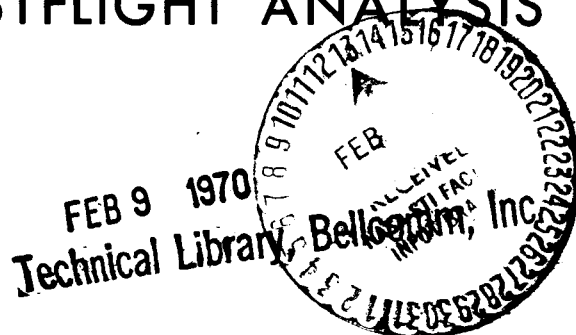
NATIONAL AERONAUTICS AND SPACE ADMINISTRATION

N.I.

MSC INTERNAL NOTE NO. 69-FM-89

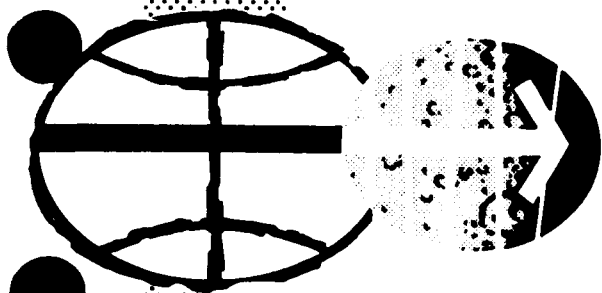
May 26, 1969

# APOLLO 7 ENTRY POSTFLIGHT ANALYSIS



Landing Analysis Branch

MISSION PLANNING AND ANALYSIS DIVISION



MANNED SPACECRAFT CENTER  
HOUSTON, TEXAS

(NASA-TM-X-69740) APOLLO 7 ENTRY  
POSTFLIGHT ANALYSIS (NASA) 38 p

N74-70628

00/99 Unclas  
16171

---

PROJECT APOLLO  
APOLLO 7 ENTRY POSTFLIGHT ANALYSIS

By Frank G. Skerbetz  
Atmospheric Flight Mechanics Section  
TRW Systems Group

---

May 26, 1969

MISSION PLANNING AND ANALYSIS DIVISION  
NATIONAL AERONAUTICS AND SPACE ADMINISTRATION  
MANNED SPACECRAFT CENTER  
HOUSTON, TEXAS

MSC Task Monitor  
D. Heath

Approved: \_\_\_\_\_

*Floyd V. Bennett*  
Floyd V. Bennett, Chief  
Landing Analysis Branch

Approved: \_\_\_\_\_

*John P. Mayer*  
John P. Mayer, Chief  
Mission Planning and Analysis Division

## CONTENTS

Section	Page
1. SUMMARY . . . . .	1
2. INTRODUCTION. . . . .	3
2.1 Purpose . . . . .	3
2.2 General Description of Contents . . . . .	3
3. SYMBOLS . . . . .	5
4. INITIAL CONDITIONS AND INPUT DATA. . . . .	7
4.1 Initial Condition State Vectors . . . . .	7
4.2 Aerodynamics Data. . . . .	7
4.3 Command Module Mass Properties . . . . .	8
4.4 Atmosphere Model . . . . .	8
5. ONBOARD SYSTEMS EVALUATION. . . . .	11
5.1 CMC Evaluation . . . . .	11
5.1.1 Guidance Phases . . . . .	11
5.1.2 Guidance Calculations. . . . .	12
5.1.3 IMU Hardware Errors . . . . .	12
5.2 Propellant Usage . . . . .	13
5.3 EMS Scroll Pattern. . . . .	14
6. ENVIRONMENT TRAJECTORY RECONSTRUCTION. . . . .	15
7. CONCLUSION . . . . .	17
REFERENCES . . . . .	33



## TABLES

Table	Page
Ia Entry State Vectors . . . . .	19
Ib CMC Initial State Vector . . . . .	20
IIa Trim Aerodynamics - Postflight . . . . .	21
IIb Trim Aerodynamics - Preflight . . . . .	21
III Comparison of Guidance State Vectors . . . . .	22
(a) Entry State Vectors . . . . .	22
(b) State Vectors at CMC Termination . . . . .	22
IV IMU Error Parameters . . . . .	23
Va Effect of Environment, Propellant System Constants, and Manual Control on Total Propellant Usage from Entry . . . . .	24
Vb Propellant Usage Per Channel . . . . .	24



## FIGURES

Figure	Page
1 Mach Number and Lift-to-Drag Ratio versus Time for Apollo 7 . . . . .	25
2 Lift-to-Drag Ratio versus Mach Number . . . . .	26
3 Load Factor versus Time for Apollo 7 . . . . .	27
4 Splashdown Coordinates for Apollo 7 . . . . .	28
5 Roll Command versus Time for Apollo 7 . . . . .	29
6 Downrange Error and Crossrange Error versus Time for Apollo 7 . . . . .	30
7 Apollo 7 Onboard Entry Monitor Scroll Trace . . . . .	31
8 Altitude Time History for Apollo 7 . . . . .	32

# APOLLO 7 ENTRY POSTFLIGHT ANALYSIS

By Frank G. Skerbetz  
Atmospheric Flight Mechanics Section  
TRW Systems Group

## 1. SUMMARY

Postflight evaluation of Apollo 7 indicated that the command module computer (CMC) performed properly throughout the entry phase of the mission and that the trajectory of the command module (CM) closely approximated calculations based upon the real-time Honeysuckle tracking vector number 769.

Performance of the CMC was evaluated by simulating the onboard guidance equations and inputting the pulse integrating pendulous accelerometer (PIPA) data recorded on the telemetry (TM) tape by the CMC. The comparison of parameters calculated by the PIPA guidance simulation (PGS) and the CMC indicated that:

- a. Each guidance logic program of the PGS phased at a time identical with the CMC programs.
- b. Differences in the state vector calculated by the PGS and the CMC increased slightly with time, indicating an accumulation of errors resulting from the accelerometer corrections and differences resulting from integration techniques.
- c. The roll commands are equivalent throughout the majority of the flight. The differences that do arise occur in the last 80 seconds of guidance calculations and are a result of the differences in state vectors mentioned above. These differences do not affect the PGS capability of guiding the CM to the target.

The CM environment trajectory was reconstructed by using the guidance commands from the PGS to control the vehicle from 0.2 g to guidance termination. This PGS environment trajectory (PET) was essentially identical to the gimbal angle environment trajectory (GAET). Both environment trajectories compared favorably with the 21-day best estimate trajectory (BET).

Both the PGS and the PET terminated close to the target point. The PGS navigation vector at guidance termination was within 0.8 nautical mile of the desired target; the PET splashdown point missed the desired target by 3.4 nautical miles.

Two unexpected events occurred during the entry phase of Apollo 7. High propellant usage was one, and the other was an irregular trace produced on the entry monitor system (EMS) scroll. The high propellant usage was simulated; however, differences do exist on a propellant per channel basis. Future postflight studies should evaluate the individual channel propellant consumption to determine if the problem is in data acquisition or math modeling. The irregular trace on the EMS scroll could not be confirmed from the TM tape data or reconstructed with post-flight simulations. This does not indicate that the load factor fluctuation was not experienced on Apollo 7, as the TM data is digital rather than analog and of a lower frequency than the EMS data.

## 2. INTRODUCTION

### 2.1 Purpose

The primary purpose of this report with regards to the task agreement (Reference 1) is twofold: (1) to evaluate the performance of the onboard systems pertaining to atmospheric flight, and (2) to reconstruct the trajectory flown by the CM from entry to splashdown.

### 2.2 General Description of Contents

A brief description of the contents of this report is presented in this section. The report is divided into three main sections: Section 4, Initial Conditions and Input Data; Section 5, Onboard Systems Evaluation; and Section 6, Environment Trajectory Reconstruction.

Section 4, Initial Conditions and Input Data, contains entry state vectors from the various sources (TM tape, BET, and tracking). The CM aerodynamics as calculated from the PIPA data, selection of the atmosphere model, and the CM mass properties are also presented and discussed.

Section 5, Onboard Systems Evaluation, compares the CMC calculations with the simulated guidance calculations. Also discussed in this section is the high propellant usage and the irregular trace on the onboard EMS scroll.

Section 6, Environment Trajectory Reconstruction, presents the reconstruction of the CM environment trajectory. This trajectory is compared to the best estimate trajectory.



### 3. SYMBOLS

ARS	Apollo reentry simulation
BET	best estimate trajectory
CM	command module
CMC	command module computer
$C_D$	aerodynamic drag coefficient
$C_L$	aerodynamic lift coefficient
DAP	digital autopilot
DRE	downrange error
EMS	entry monitor system
GAET	gimbal angle environment trajectory
g. e. t.	ground elapsed time
G&N	guidance and navigation
IMU	inertial measurement unit
L/D	aerodynamic lift-to-drag ratio
PET	PIPA environment trajectory
PGS	PIPA guidance simulation
PIPA	pulse integrating pendulous accelerometer
RCS	reaction control system
SM	service module
TM	telemetry
P61	Entry Preparation Program
P62	CM/SM Separation and Preentry Maneuver Program
P63	Entry Initialization Program

P64 Post 0.5 g Program

P67 Final Phase Program

c. g.	center of gravity
cm/sec <sup>2</sup>	centimeters per second per second
deg	degree
ft	feet
ft/sec	feet per second
g	acceleration of gravity
hr:min:sec	hours: minutes: seconds
lb	pound
meru	milli earth rate unit
meru/g	milli earth rate unit per acceleration of gravity
n mi	nautical mile
sec	second

## 4. INITIAL CONDITIONS AND INPUT DATA

This section presents the initial condition state vectors and input data used in postflight analysis of Apollo 7. Input data presented in this section are the CM aerodynamics, the CM mass properties, and atmosphere selection.

### 4.1 Initial Condition State Vectors

Three entry state vectors were used in postflight studies. One was obtained from the Corpus Christi Tracking Station. This vector does not include data from any other tracking station. The second entry state vector came from the BET, and the third was obtained from the TM tape. These vectors and the entry state vector based on real-time calculations are presented in Table Ia. The three postflight entry vectors are in good agreement with the real-time vector, and no significant trajectory differences arise from initializing with any postflight entry vector.

At approximately 259 hours, 43 minutes, and 36 seconds, ground elapsed time, the separation maneuver between the CM and the service module (SM) was performed. All postflight reconstruction involving the CMC was initialized at this time with the state vector presented in Table Ib.

### 4.2 Aerodynamic Data

Postflight lift-to-drag (L/D) ratios were calculated by the CMC by the method presented in Reference 2. Figure 1 presents a time history of the L/D values as calculated by the CMC from the PIPA counts. A 6-D guidance and navigation (G&N) trajectory simulation using preflight aerodynamic data from Reference 3 was used to correlate Mach number to time. This correlation is presented in Figure 1. These two time histories were used to derive L/D as a function of Mach number. Trim angle of attack and coefficient of drag ( $C_D$ ) as functions of Mach number were also obtained from the 6-D simulation. The coefficient of lift ( $C_L$ ) was calculated as a function of Mach number as the product of L/D and  $C_D$ .

Table IIa presents the postflight trim aerodynamics, and Table IIb presents the preflight trim aerodynamics. Figure 2 compares the preflight and postflight L/D as a function of Mach number.

Comparison of the data presented indicates that the postflight L/D was on the average slightly lower than expected in the Mach number region from 4.0 to 29.0 and was higher than expected for Mach numbers less than 4.0. However, in general, the postflight aerodynamic data were in good agreement with preflight predictions (within the three sigma  $\pm 0.03$  variation).

#### 4.3 Command Module Mass Properties

The mass properties presented below are from Reference 4 and represent the vehicle characteristics after CM/SM separation. The CM weight was 12,364.1 pounds. This is 8.1 pounds heavier than the pre-flight estimated value. The center-of-gravity locations in the Apollo body axis coordinate system in inches are:

$$X = 1040.8$$

$$Y = -0.2$$

$$Z = 6.0$$

The CM moments and products of inertia are listed below in units of slug - feet squared:

$$I_{xx} = 5799. \quad I_{xy} = 42.$$

$$I_{yy} = 5213. \quad I_{xz} = -423.$$

$$I_{zz} = 4745. \quad I_{yz} = 30.$$

#### 4.4 Atmosphere Model

The atmosphere model chosen for the reconstruction was the 30° North, July atmosphere, as defined in Reference 5. The selection of this atmosphere was based on the best load-factor time history of a gimbal angle driven environment trajectory, the miss distance of the trajectory and time of drogue deployment.

The GAET used gimbal angle as recorded on the TM tape. The gimbal angles were input directly into the trajectory equations thus eliminating nonenvironment parameters such as the guidance commands and the response and execution of the digital autopilot (DAP).

The load factor time history resulting from the 30° North, July atmosphere, is compared to the BET in Figure 3. The BET reached 0.05 g at approximately 935,737.0 seconds, ground elapsed time, as compared to 935,735.0 seconds for the GAET. Both the BET and the GAET had two maxima on the load factor time history. For the BET the first peak of 3.20 g occurred at approximately 936,015.0 seconds, ground elapsed time; the second was 3.28 g in magnitude and occurred at 936,070.0 seconds. The first peak of the GAET occurred at 936,020.0 seconds and was 3.39 g. The second peak of 3.29 g occurred at approximately 936,065.0 seconds, ground elapsed time.

All atmospheres investigated produced similar load factor time histories with a peak load factor of approximately 3.4 g near 936,020.0 seconds, ground elapsed time. The deciding factor, then, became the miss

distance and time at drogue chute deployment. The GAET, using the 30° North, July atmosphere, missed the desired target by 1.7 nautical miles. The GAET coordinates at drogue deployment along with the desired target is presented in Figure 4. The GAET time of drogue deployment differed from the BET by approximately 8.0 seconds.

The agreement between the load factor time history and the coordinates at drogue deployment indicated that the 30° North, July atmosphere, coupled with the aerodynamic data presented in Section 3.2 represented a good estimate of the conditions present during the Apollo 7 entry.



## 5. ONBOARD SYSTEMS EVALUATION

Performance of the CMC is discussed in this section. The high propellant usage and the irregular load factor trace on the EMS scroll are also discussed.

### 5.1 CMC Evaluation

Presented within this section are the results of the CMC evaluation. This evaluation showed that the CMC performed as expected during the Apollo 7 entry phase.

The methods and data used in evaluating the performance of the CMC are discussed together with comparisons of the PIPA guidance simulation (PGS) and the CMC. Specific evaluation parameters were time of transfer into the various guidance phases and significant events which occurred during the phases. Other evaluation considerations were CMC computed state vectors, roll commands, ranging errors, and general trajectory parameters. The inertial measurement unit (IMU) errors, determined in the BET generation, were used to compute CMC dispersions at touchdown.

The operation of the CMC was simulated using the PIPA external drive option of the Apollo Reentry Simulation (ARS). PIPA data recorded on the TM tape at 2-second intervals by the CMC were input to the simulated CMC logic of ARS as a means of reconstructing the CMC's performance. In order to provide the PIPA driven guidance simulation with approximately the same initialization as the onboard CMC, the PGS was initialized at 935,016.0 seconds, ground elapsed time, using the state vector presented in Table Ib.

5.1.1 Guidance phases. - The Apollo 7 entry trajectory required the use of five of the seven guidance programs. The Entry Preparation Program (P61) was initiated at 934,823.0 seconds, ground elapsed time. Separation of the CM from the SM occurred during P61, approximately 3 minutes and 13 seconds after P61 initiation. The CM/SM Separation and Preentry Maneuver Program (P62) initiated at 935,060.0 seconds and terminated at 935,078.0 seconds after properly aligning the CM for entry. At 935,078.0 seconds the CMC transferred into the Entry Initialization Program (P63). Time of entrance into the remaining two guidance programs, Post 0.5 g (P64) and Final Phase (P67), was the first comparison in evaluating the CMC's performance. The first record in each program from both the CMC and the PGS occurred at identical times indicating that both guidance routines initiated the two phases within the same 2-second computing cycle as listed below:

<u>Guidance Phase</u>	<u>Phase Initialization Time (hr:min:sec)(g. e. t.)</u>
Program 64	259:55:40
Program 67	259:56:06

5.1.2 Guidance calculations. - The data computed by the PGS were in good agreement with the data recorded on the TM tape. CMC and PGS calculations used in the comparisons to evaluate performance were state vectors, roll commands, downrange error (DRE), and crossrange error.

Table III presents a comparison of the integrated state vectors at entry (Table IIIa) and at guidance termination (Table IIIb). The state vectors are essentially identical at entry with the very minor difference in altitude of 180.0 feet being the largest difference. Larger deviations at guidance termination are the result of an accumulation of small differences throughout the entry portion of the flight. These state vectors are in good agreement.

The integrated state vectors are then used by the guidance logic to calculate roll commands. Figure 5 presents the roll commands calculated by both the CMC and PGS. From 0.2 g until 936,060.0 seconds, ground elapsed time, comparison shows the roll commands to be identical. At 936,060.0 seconds, the accumulation of errors becomes significant and the magnitude of the PGS commands diverges from the CMC commands; however, the roll command reversals occur at approximately the same time. With this divergence, the PGS calculations terminated within approximately 0.8 nautical mile of the desired target. This termination point is shown in Figure 4.

Simulations were initiated using a TM state vector in the regions where the roll commands diverge in an effort to explain this divergence. These simulations did not contain the accumulation of small differences present in the PGS at the time divergence occurred, and roll commands similar to the CMC roll commands were calculated. Simulation results prove conclusively that the roll command divergence is a result of the accumulation of small differences in the PGS and was not the result of errors in the CMC calculations of roll command.

The final calculations used to evaluate the onboard guidance were the DRE and crossrange error. Figure 6 shows excellent agreement between the CMC and PGS ranging error calculations.

5.1.3 IMU hardware errors. - An influencing factor on the guidance calculations was the errors present in the guidance hardware, i. e., accelerometer and platform errors. An estimate of the errors present in Apollo 7 was made prior to entry. This preentry estimate was incorporated in the guidance calculations during entry and is reflected in the PIPA data recorded on the TM tape.

Postflight evaluation (Reference 6) concluded that the preentry IMU error estimates differed from the errors present during entry. These differences are listed in Table IV. All postflight errors are within the standard deviation (Reference 6), except the gyro-bias drift in the Y-axis and the input axis acceleration sensitivity drift in the X- and Z-axes. However, these three errors are not significantly larger than the standard deviation.

The effect of the postflight IMU error corrections, when included in the guidance postflight analysis, result in a downrange error of 0.006 nautical mile and a lateral miss distance which differed by 0.167 nautical mile from the postflight guidance reconstruction without IMU error corrections.

The table below presents comparisons of onboard velocity, altitude, and altitude rate taken at the time of entry (935,608.05 seconds, g. e. t.), CMC termination (936,140.0 seconds, g. e. t.), and time of drogue deployment (936,210.0 seconds, g. e. t.) based on the TM tape data, with post-flight guidance simulations and the BET. These comparisons indicate that the effect of IMU errors on the guidance calculations are small. The altitude difference at drogue deployment between all guidance simulations and the BET is the result of the 2,279-foot altitude difference at entry and the 5.9 foot-per-second altitude rate difference at entry.

<u>Event</u>	<u>Time (sec, g. e. t.)</u>	<u>Source</u>	<u>Velocity (ft/sec)</u>	<u>Altitude (ft)</u>	<u>Altitude Rate (ft/sec)</u>
Entry	935, 608.	Command Module Computer	25,848.6**	399,902.	-923.6
		Guidance reconstruction without IMU errors	25,848.3**	400,081.	-922.9
		Guidance reconstruction with IMU errors	25,848.3**	400,081.	-922.9
		Best Estimate Trajectory	25,848.5**	397,802.	-928.8
CMC termination	936, 140.	Command Module Computer	967.6*	69,126.	-796.4
		Guidance reconstruction without IMU errors	966.1*	69,899.	-795.8
		Guidance reconstruction with IMU errors	970.6*	68,757.	-799.7
		Best Estimate Trajectory	990.7*	62,772.	-806.4
Drogue chute deployment	936, 206.	Command Module Computer	362.5*	31,373.	-352.8
		Guidance reconstruction without IMU errors	361.6*	32,188.	-352.0
		Guidance reconstruction with IMU errors	365.9*	31,325.	-357.7
		Best Estimate Trajectory	385.6*	23,708.	-365.3

\* Relative velocity

\*\* Inertial velocity

## 5.2 Propellant Usage

One unexpected event of the Apollo 7 entry trajectory was the high propellant usage. Based upon the best available preflight predictions, 26.7 pounds of propellant were assumed sufficient for a G&N entry using only one reaction control system (RCS). This mission, however, used 47.1 pounds from separation to splashdown. The excessive propellant usage can mostly be attributed to using both RCS rings for the last 4 minutes and 40 seconds of the flight. Other contributing factors were the high winds that were prevalent (Reference 7), the specific atmosphere, and manually maneuvering the CM to a bank angle of -55.0 degrees and maintaining this attitude for approximately 80 seconds.

A 6-D simulation including all of the factors mentioned above produced a total propellant usage of 47.48 pounds. Table Va shows the contribution of each of the above factors to the total propellant usage. Each simulation listed in Table Va is an accumulation of the previous simulations. The greatest contribution to the excessive amount of propellant used was the use of the two RCS rings. This accounted for 17.3 pounds of propellant. The atmosphere effect reduced the amount of propellant needed by approximately 2.1 pounds. Manual maneuvering and maintaining a bank angle of -55.0 degrees required approximately 1.3 pounds. The effects of the wind velocity-altitude profile increased the amount of propellant needed by approximately 4.3 pounds.

An externally driven 6-D simulation produced a total propellant usage of 52.6 pounds. This simulation was driven by the roll commands recorded on the TM tape and includes all conditions present in the above simulations. This simulation is also listed in Table Va.

Table Vb breaks the total propellant usage down into the individual channels for both the A and B propellant systems. The 6-D G&N simulation indicates that postflight simulations reconstructed the high propellant usage using the actual flight conditions. This reconstruction, however, is low in the plus pitch and both yaw channels and high in the negative pitch and both roll channels.

The roll command drive propellant usage is also presented in Table Vb. The predications of this simulation are low in both pitch and high in both yaw and both roll channels.

It can be concluded from this brief investigation that a detailed investigation is required to effectively determine and then simulate the propellant consumption of the CM/RCS system.

### 5.3 EMS Scroll Pattern

Another peculiarity of Apollo 7 was the irregular trace on the EMS scroll. The trace varied by approximately as much as  $\pm 0.05$  g about the mean in a sinusoidal pattern throughout most of the trajectory. This fluctuation is shown in Figure 7. The load factors from the PIPA environment trajectory, the gimbal angle environment trajectory, and the drag from the PIPA guidance simulation were identical in magnitude with the mean of the EMS trace but these simulations did not show the sinusoidal variation. These observations plus the fact that the load factor variation was not evident in the PIPA data indicate that the EMS load factor fluctuation could not be confirmed from postflight TM data which are available at 2-second intervals. The data from the EMS accelerometer are the result of a continuous analog signal and this continuous signal may have sensed a load factor fluctuation not evident on the TM tape.

A second abnormality of the EMS was the malfunction of the range counter. The malfunction was detected prior to launch and the range counter failed all subsequent testing.

## 6. ENVIRONMENT TRAJECTORY RECONSTRUCTION

This section presents and discusses the PIPA environment trajectory (PET) resulting from the PIPA driven guidance simulation. Also presented in this section is the gimbal angle driven environment trajectory (GAET) previously discussed in Section 4.4. The GAET is included in this section to show the comparison of both postflight environment trajectories to the BET as well as to each other.

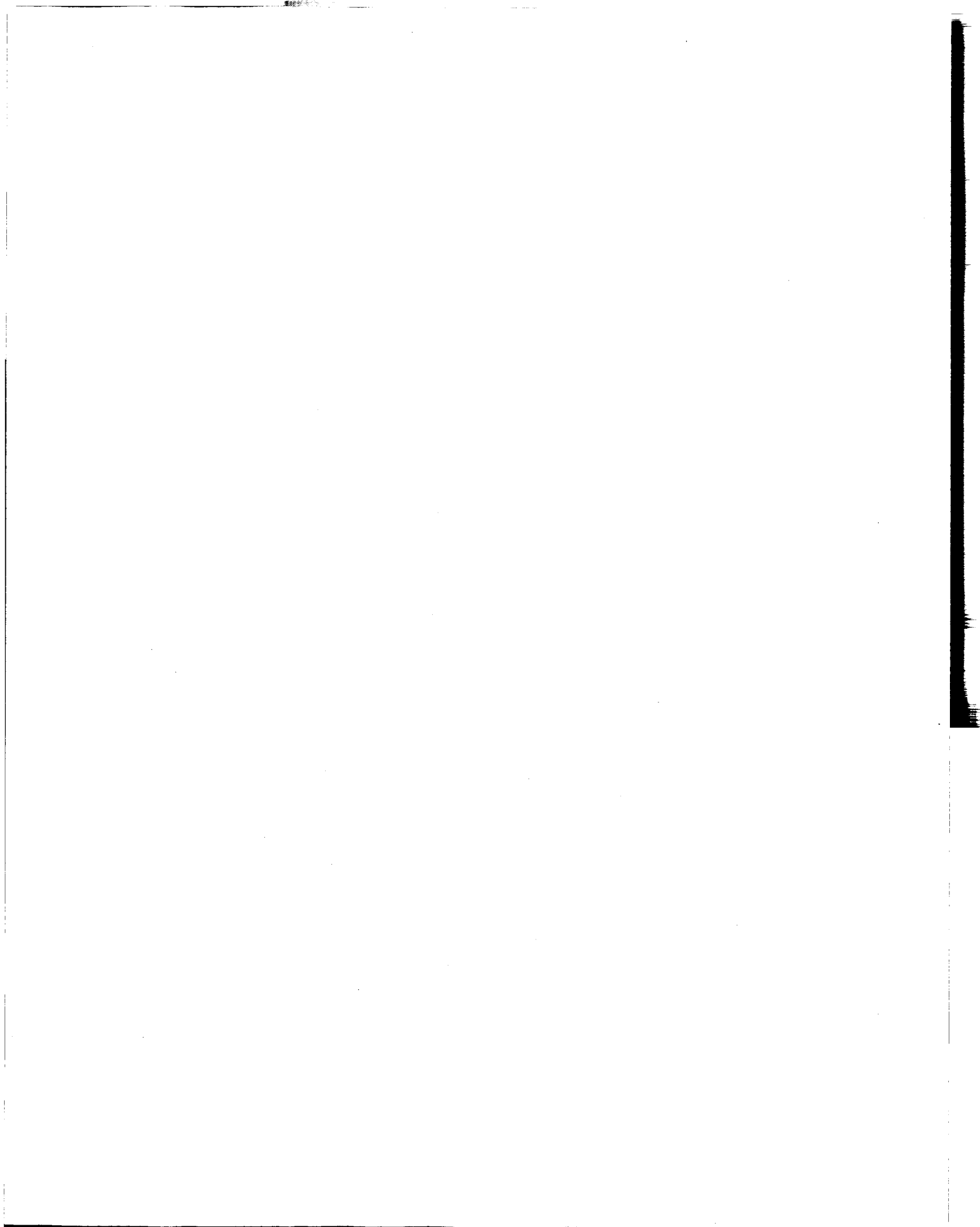
The PET was a result of simulating the onboard guidance calculations and DAP. The roll commands calculated by the PIPA driven guidance simulation (PGS)(discussed in Section 5.1) were used to drive the PET to the desired target. The proper environment and CM data as described in Section 4 were also included in this reconstruction.

The load factor time history of the PET is compared to the BET in Figure 3. The maximum load factor for this trajectory was 3.36 g and occurred at 936,062.0 seconds, ground elapsed time. This maximum load factor occurred 8 seconds earlier than the BET and was 0.08 g greater in magnitude. The maximum load factor of 3.39 g on the GAET was experienced 50 seconds earlier than the BET maximum.

Figure 4 presents the splashdown coordinates for the PET. The miss distance of 3.4 nautical miles is in good agreement with the other postflight simulations. The comparatively large miss distance of the United States Navy estimated splashdown point relative to the target (approximately 8.0 nautical miles not including a  $\pm 3.0$ -nautical mile uncertainty) does not agree with any postflight simulation or the CMC.

Figure 8 presents the altitude time history of the BET in addition to the altitude difference of both the GAET and PET from the BET. The maximum deviation of the GAET, -6400 feet, occurs at approximately 936,140.0 seconds, ground elapsed time. Initially the PET altitude difference follows the GAET trend, but at 936,080.0 seconds the two curves diverge resulting in a maximum deviation of approximately 6,800.0 feet at 936,170.0 seconds. Also at 936,080.0 seconds, roll commands from the PGS began to differ from the CMC calculations and the near full lift up commands forced the PET altitude to decrease at a rate slower than the BET which resulted in the positive altitude difference. The altitude differences are small considering the different methods from which each was calculated, and they caused no serious trajectory differences.

Both the PET and GAET are in good agreement with the BET. The differences between the PGS and the CMC calculations discussed in Section 5.1 became evident in the PET. This difference, however, caused no serious trajectory deviations.



## 7. CONCLUSIONS

Postflight evaluation of the CMC indicated that the CMC performed as expected. The DRE at 0.2 g was well within the tolerance allotted for a G&N entry. The entry guidance program phasing occurred within the same 2-second computation cycle as did the CMC simulation; the difference between the CMC calculated navigation vectors and the simulated vectors is small; and the roll commands are equivalent through the initial portion of the trajectory and result in splashdown coordinates within 3.0 nautical miles of target.

The irregular trace on the EMS scroll was not evident in postflight analysis. This does not confirm that the CM did not experience the load factor fluctuation as postflight data are only available at 2-second intervals. The high propellant usage was reconstructed; however, the additional investigations are required to predict accurately the propellant consumption of each channel.

The CM reconstructed entry trajectory, the PIPA environment trajectory, compared favorably with both the gimbal angle environment trajectory and the best estimate trajectory.

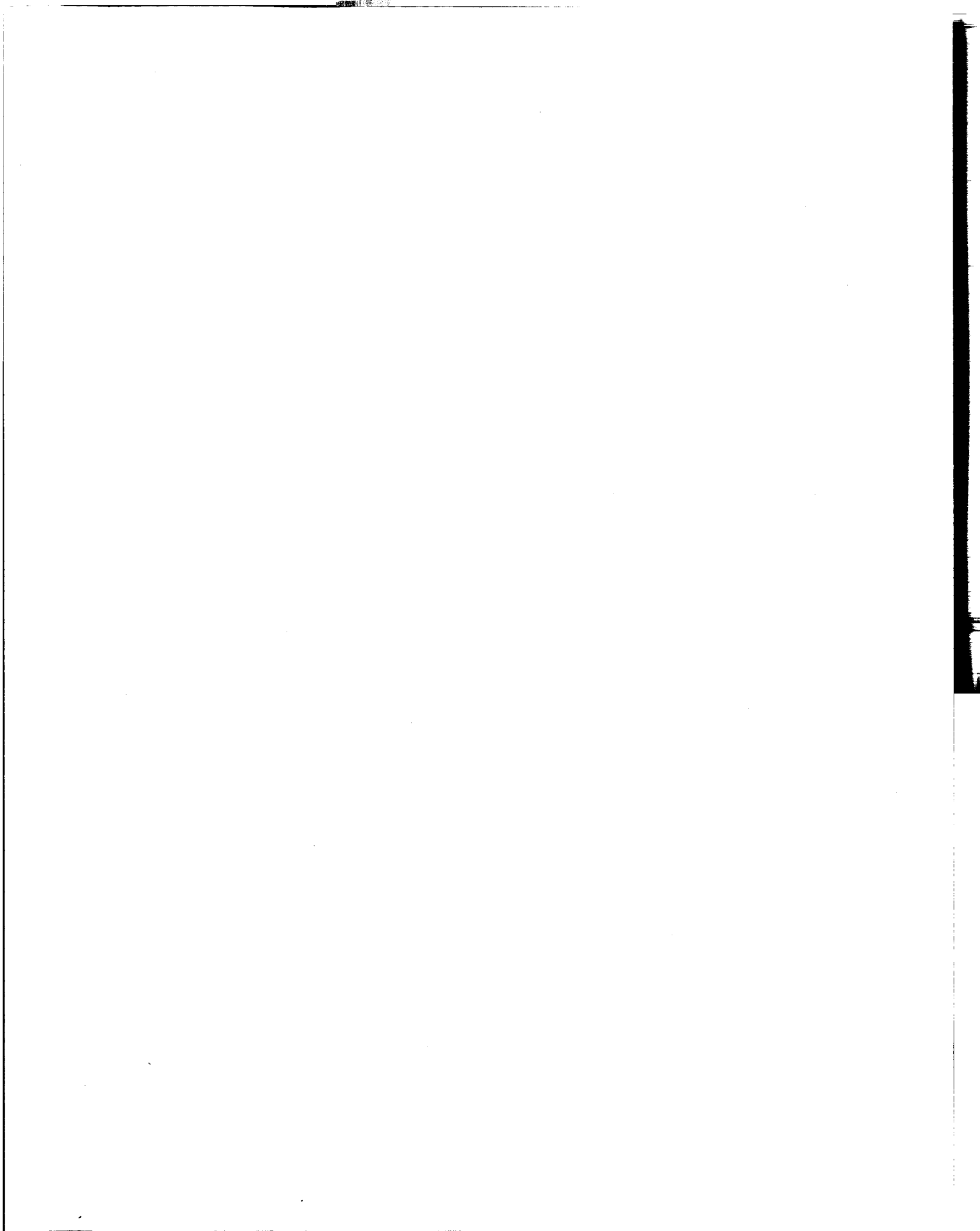


Table Ia. Entry State Vectors

	<u>BET</u>	<u>Corpus Christi Tracking Vector</u>	<u>TM (Entry)</u>	<u>Real Time</u>
Time (sec)	935,608	935,608.	935,608.	935,608.
Geodetic latitude (deg)	29.926	29.921	29.923	29.922
Longitude, West (deg)	92.444	92.520	92.431	92.502
Altitude (ft)	397,802.1	397,214.5	399,901.8	398,136.6
Inertial velocity (ft/sec)	25,848.512	25,848.230	25,848.597	25,846.525
Inertial flight- path angle (deg below local hor- izontal)	2.055	2.066	2.047	2.061
Inertial azimuth (deg)	87.552	87.511	87.560	87.520
*X (ft)	20,313,671.	20,320,477.	20,314,447.	20,319,986.
*Y (ft)	-126,435.	-126,939.	-126,287.	-126,924.
*Z (ft)	6,425,960.	6,401,326.	6,430,460.	6,407,038.
* $\dot{X}$ (ft/sec)	-8,674.399	-8,649.783	-8,675.836	-8,653.311
* $\dot{Y}$ (ft/sec)	90.807	90.034	91.930	90.323
* $\dot{Z}$ (ft/sec)	24,357.423	24,348.950	24,348.950	24,354.772

\*Terms are measured in platform coordinates.

Table Ib. CMC Initial State Vector

---

	TM (Initialization)
Time (sec)	935,016.
Geodetic latitude (deg)	20.965
Longitude, West (deg)	133.445
Altitude (ft)	943,729.5
Inertial velocity (ft/sec)	25,196.638
Inertial flight-path angle (deg below local horizontal)	1.969
Inertial azimuth (deg)	68.106
*X (ft)	20,194,896.
*Y (ft)	-139,745.
*Z (ft)	-8,368,420.
* $\dot{X}$ (ft/sec)	8,839.886
* $\dot{Y}$ (ft/sec)	-45.608
* $\dot{Z}$ (ft/sec)	23,595.020

---

\*Terms are measured in platform coordinates.

Table IIa. Trim Aerodynamics - Postflight

<u>Mach Number</u>	<u>C<sub>L</sub></u>	<u>C<sub>D</sub></u>	<u>Trim Angle of Attack (deg)</u>	<u>L/D</u>
0.688	0.205798	0.97999	164.634	0.210
0.942	0.323335	1.09605	158.618	0.295
1.618	0.582135	1.26551	153.177	0.460
3.344	0.448758	1.21286	154.665	0.370
3.375	0.433901	1.21541	156.201	0.357
8.551	0.423257	1.21976	156.506	0.347
11.227	0.423039	1.22620	156.877	0.345
13.373	0.409476	1.23336	157.239	0.332
15.284	0.402916	1.23974	157.561	0.325
17.163	0.402461	1.24601	157.878	0.323
19.161	0.394594	1.25268	158.216	0.314
21.156	0.386617	1.25934	158.552	0.307
23.316	0.392634	1.26656	158.917	0.310
25.463	0.388486	1.27372	159.279	0.305
27.720	0.404880	1.28126	159.660	0.316

Table IIb. Trim Aerodynamics - Preflight

<u>Mach Number</u>	<u>C<sub>L</sub></u>	<u>C<sub>D</sub></u>	<u>Trim Angle of Attack (deg)</u>	<u>L/D</u>
0.40	0.24399	0.8531	167.17	0.2860
0.70	0.26368	0.9852	164.53	0.2676
1.10	0.49540	1.1684	154.76	0.4240
1.20	0.48008	1.1548	155.03	0.4157
1.35	0.56442	1.2776	153.92	0.4418
1.65	0.55160	1.2641	153.09	0.4364
2.00	0.53387	1.2689	152.97	0.4207
2.40	0.50892	1.2378	153.45	0.4111
3.00	0.48036	1.2131	153.97	0.3960
4.00	0.44293	1.2124	155.99	0.3653
10.00	0.42994	1.2221	156.67	0.3518
27.72	0.39208	1.2813	159.66	0.3060

Table III. Comparison of Guidance State Vectors

Table IIIa. Entry State Vectors

	<u>TM Tape</u>	<u>PIPA Guidance Simulation</u>	<u>Best Estimate Trajectory</u>
Time (hr:min:sec)	259:53:28	259:53:28	259:53:28
Latitude (deg)	29.923	29.923	29.926
Longitude, West (deg)	92.431	92.431	92.444
Altitude (ft)	399,901.	400,081.	397,802.
Inertial velocity (ft/sec)	25,848.6	25,848.3	25,848.5
Inertial flight-path angle (deg below local horizontal)	2.047	2.046	2.055
Inertial azimuth (deg)	87.560	87.560	87.552

Table IIIb. State Vectors at CMC Termination

	<u>TM Tape</u>	<u>PIPA Guidance Simulation</u>	<u>Best Estimate Trajectory</u>
Time (hr:min:sec)	260:02:20	260:02:20	260:02:20
Latitude (deg)	27.629	27.630	27.633
Longitude, West (deg)	64.182	64.187	64.192
Altitude (ft)	69,126.7	69,899.0	62,772.3
Inertial velocity (ft/sec)	2,043.4	2,041.7	2,050.4
Inertial flight-path angle (deg below local horizontal)	22.937	22.942	23.433
Inertial azimuth (deg)	97.344	97.340	97.316

Table IV. IMU Error Parameters

<u>Error Source</u>	<u>Axis</u>	<u>Errors</u>
Accelerometer bias (cm/sec <sup>2</sup> )	X	0.036
	Y	-0.028
	Z	0.010
Accelerometer scale factor (parts/million)	X	50.0
	Y	0.0
	Z	-84.0
Gyro - bias drift (meru)	X	1.02
	Y	4.13
	Z	0.00
Input axis acceleration sensitivity drift (meru/g)	X	-12.0
	Y	4.1
	Z	-10.5
Input axis acceleration sensitivity drift (meru/g)	X	1.24
	Y	0.0
	Z	0.0
Gyro misalignment (arc sec)	X	39.0
	Y	-50.0
	Z	-25.0

Table Va. Effect of Environment, Propellant System Constants, and Manual Control on Total Propellant Usage from Entry

<u>Simulation Description</u>	<u>Propellant (lb)</u>
6-D, G&N entry, standard atmosphere, Apollo 7 mass properties, one fuel system	26.7
Manual maneuvering	28.0
Phasing of second propellant system	45.3
30° North - July atmosphere	43.2
Wind data	47.5
Roll command drive	52.6

Note: Each simulation is an accumulation of data from the previous simulations.

Table Vb. Propellant Usage Per Channel

<u>System</u>	<u>Simulation</u>	<u>Propellant Usage Per Engine (lb)</u>						<u>Total</u>
		<u>+Pitch</u>	<u>-Pitch</u>	<u>+Yaw</u>	<u>-Yaw</u>	<u>+Roll</u>	<u>-Roll</u>	
A	Actual	1.19	4.03	2.01	2.55	9.03	8.30	27.11
	6-D G&N	0.25	5.39	0.93	0.43	10.59	10.98	28.57
	Roll	0.25	0.45	2.75	6.04	9.57	10.05	29.11
	command							
B	Actual	1.22	3.50	2.04	2.70	5.81	4.72	19.99
	6-D G&N	0.00	4.97	0.58	0.04	6.53	6.79	18.91
	Roll	0.00	0.45	2.64	6.04	6.96	7.40	23.49
	command							
<u>Total</u>								
Actual		47.10						
6-D G&N		47.48						
Roll command		52.60						

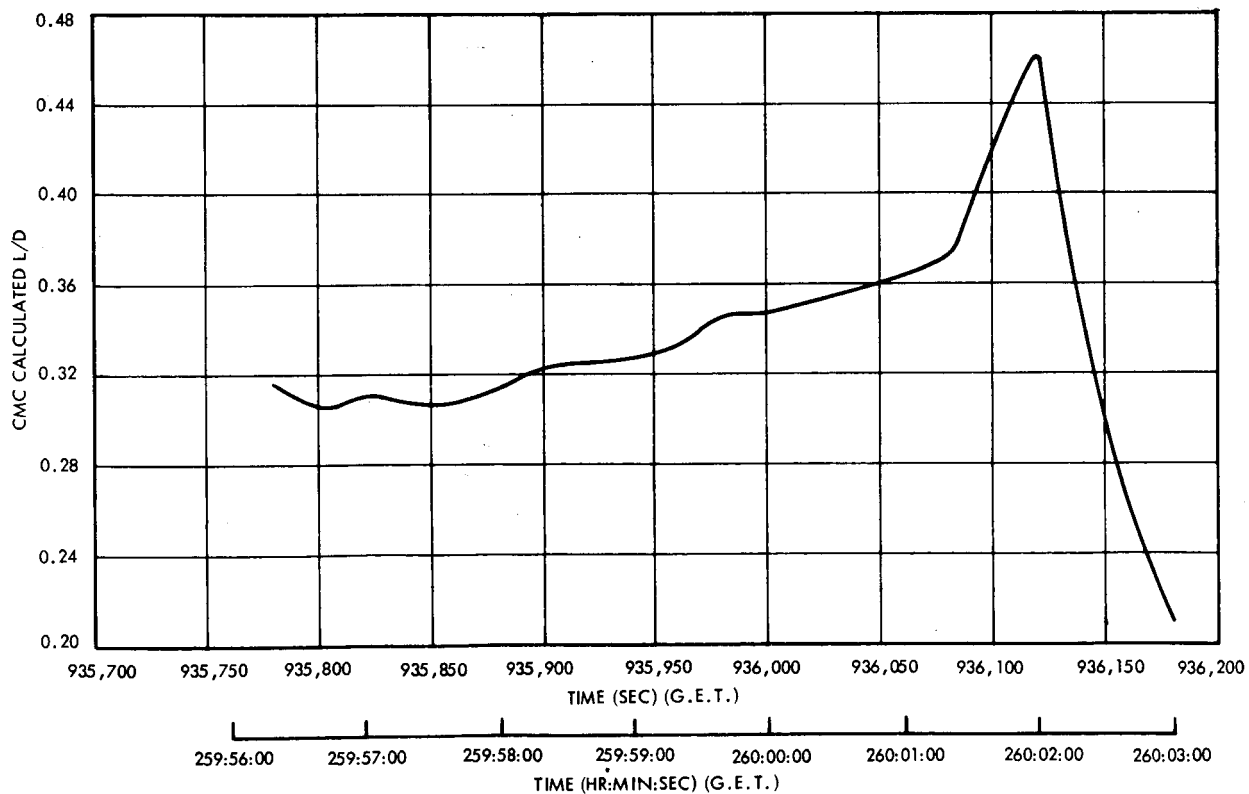
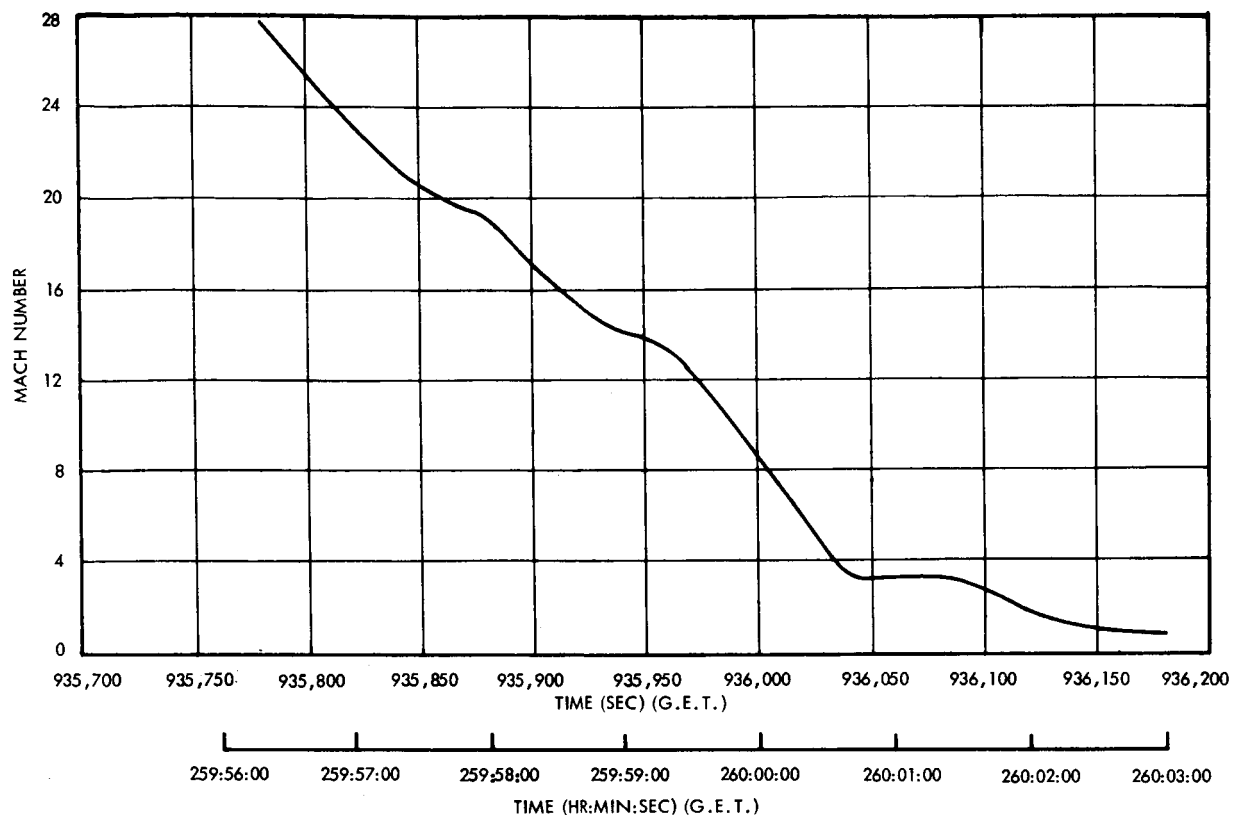


Figure 1. Mach Number and Lift-to-Drag Ratio versus Time for Apollo 7

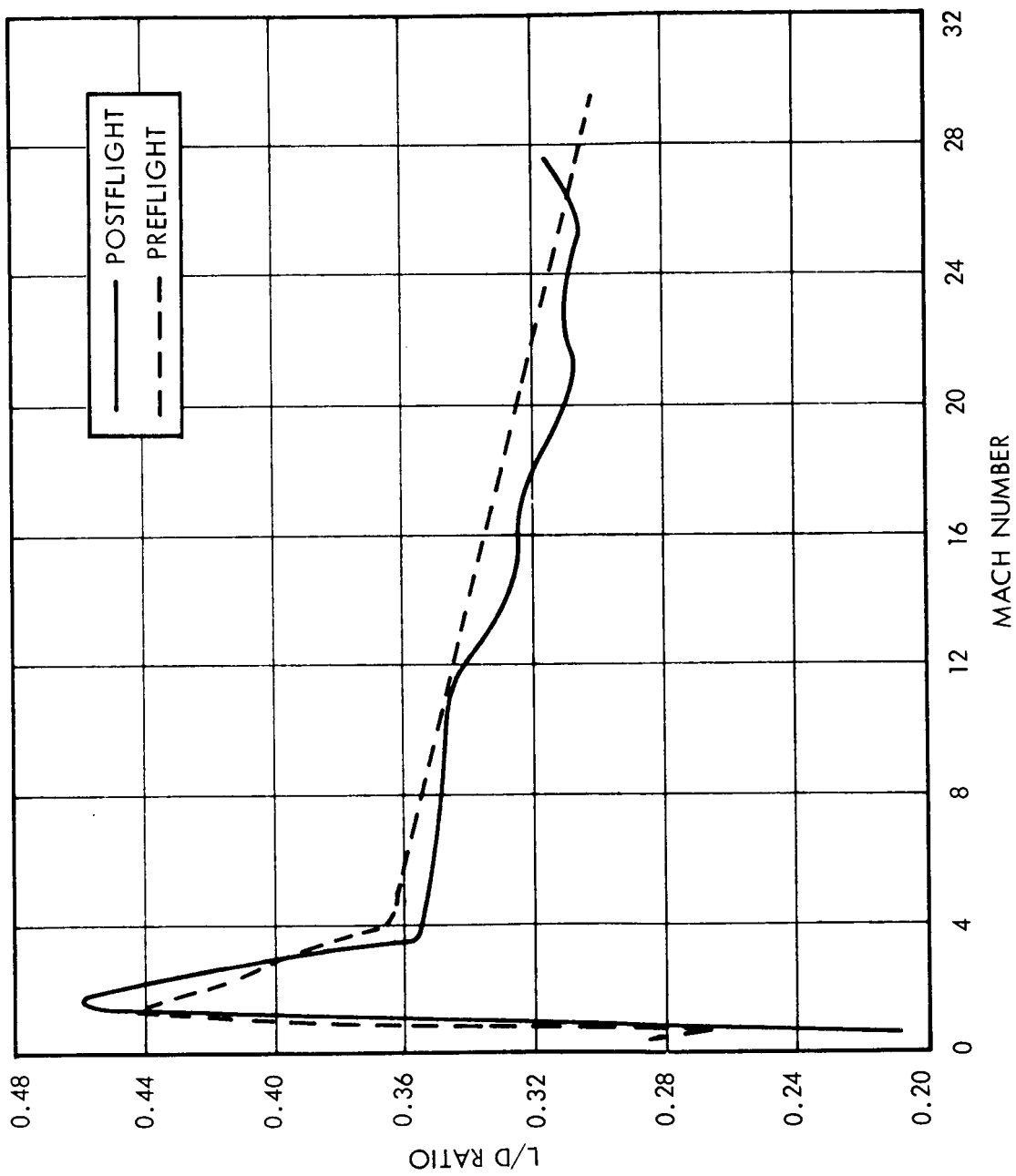


Figure 2. Lift-to-Drag Ratio versus Mach Number

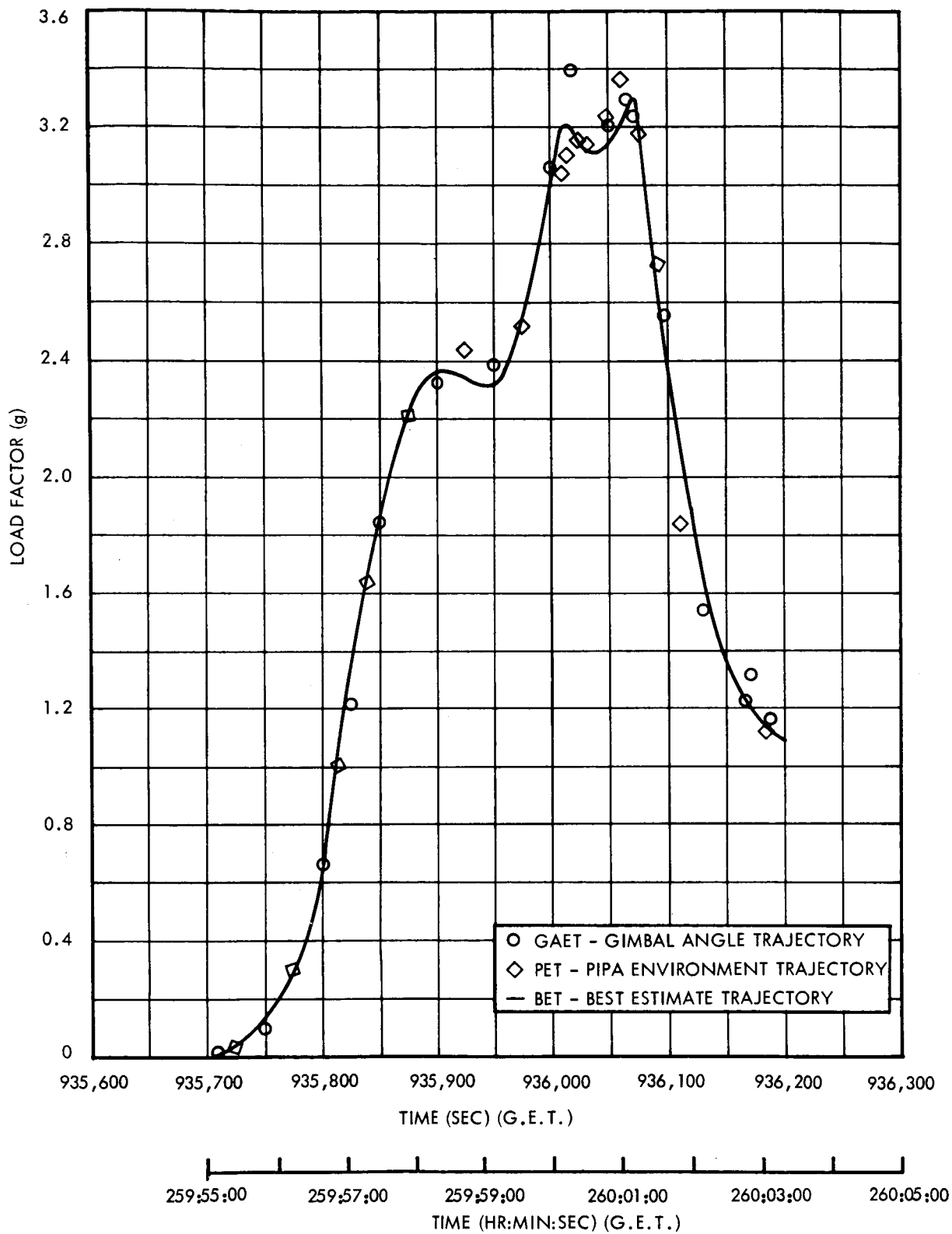


Figure 3. Load Factor versus Time for Apollo 7

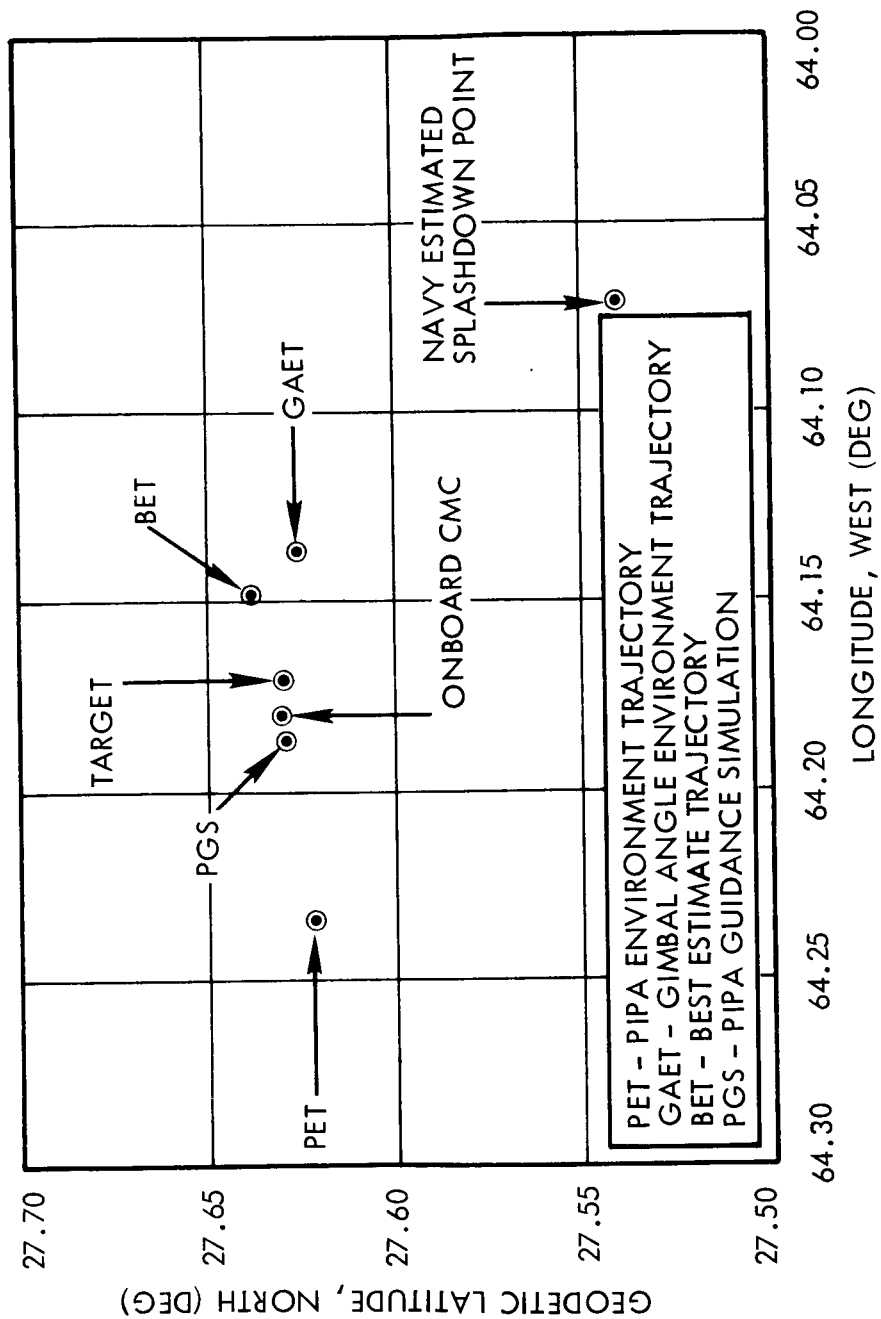


Figure 4. Splashdown Coordinates for Apollo 7

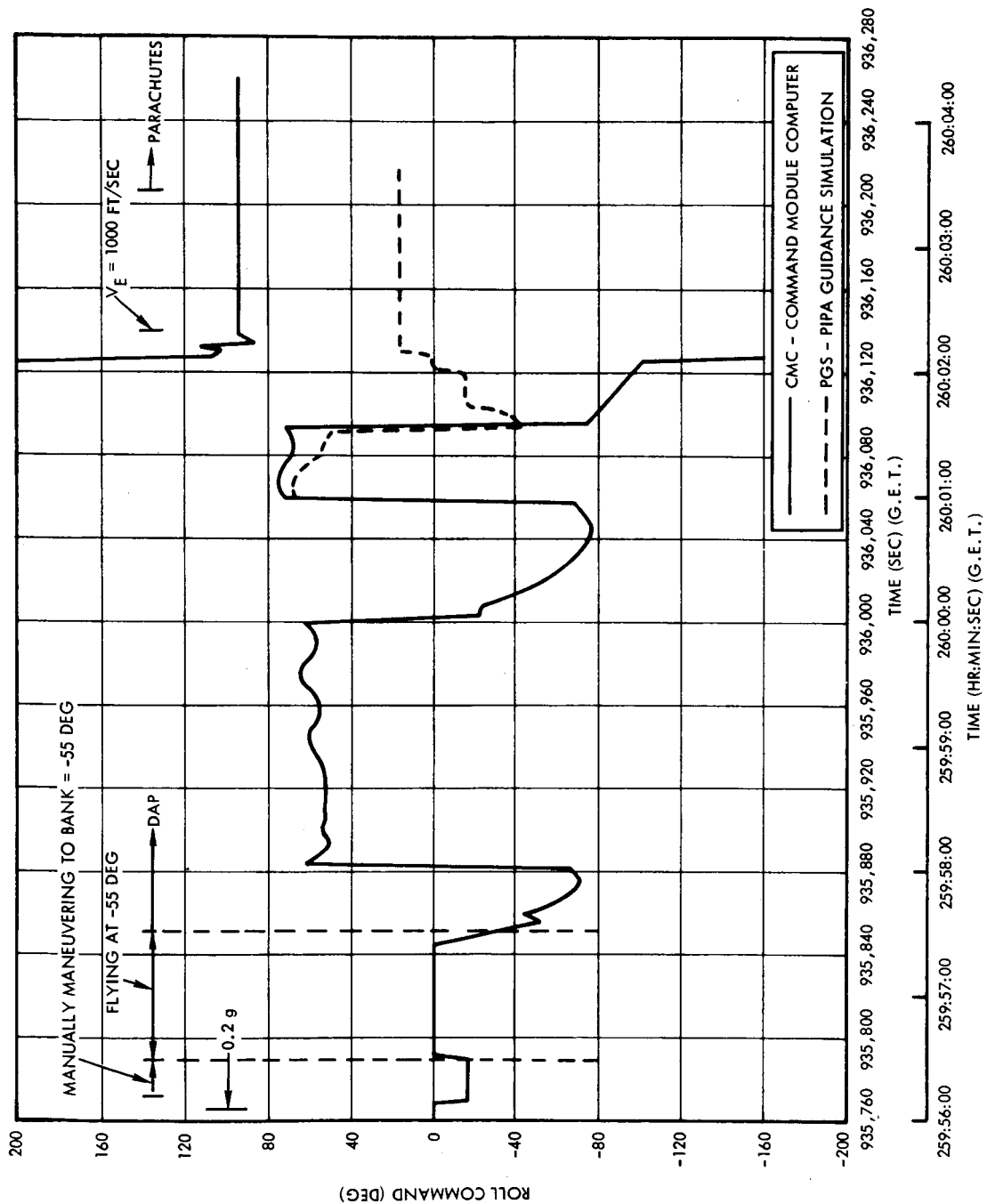


Figure 5. Roll Command versus Time for Apollo 7

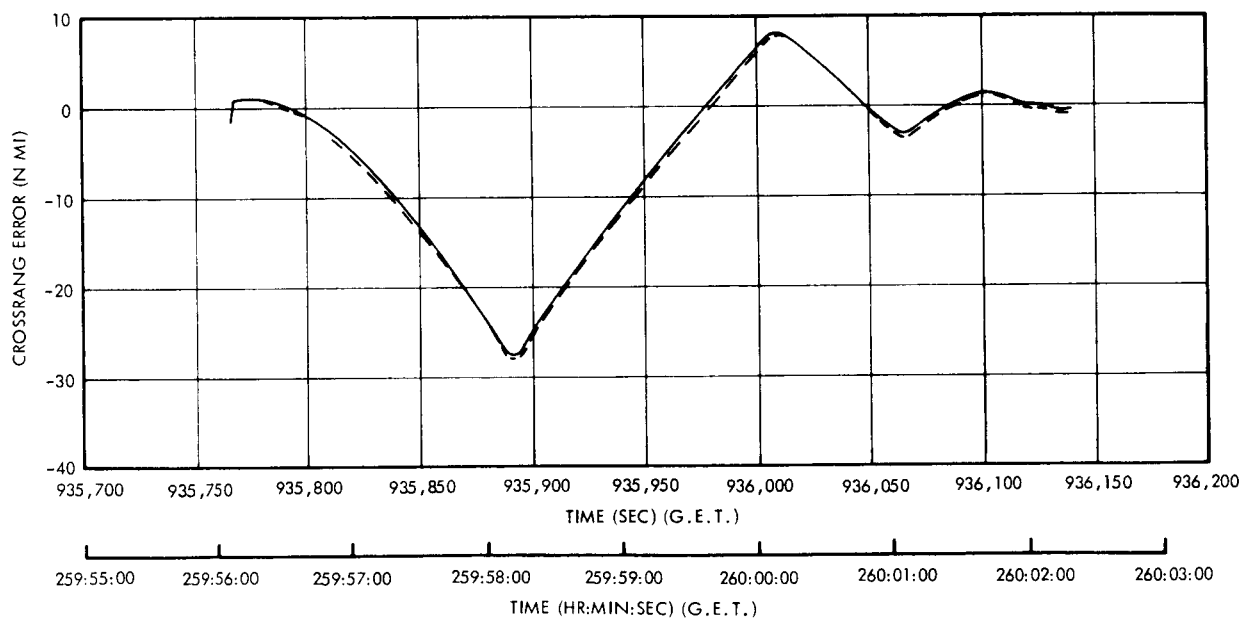
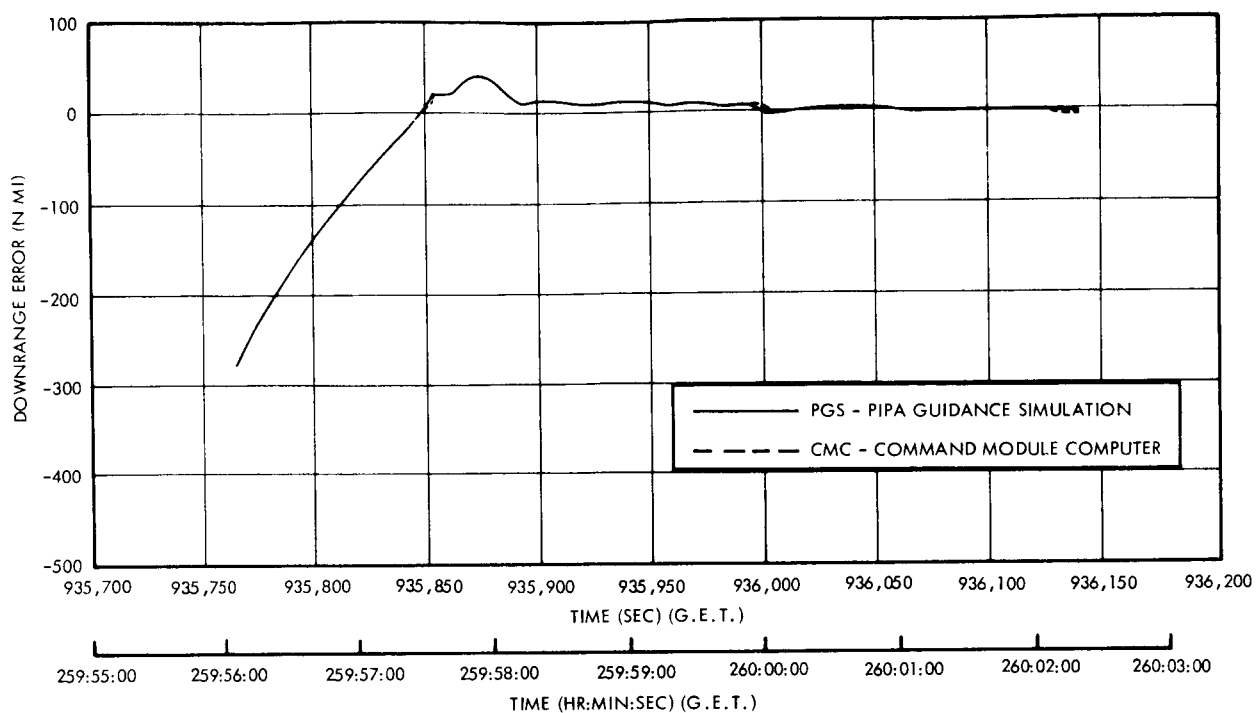


Figure 6. Downrange Error and Crossrange Error  
versus Time for Apollo 7

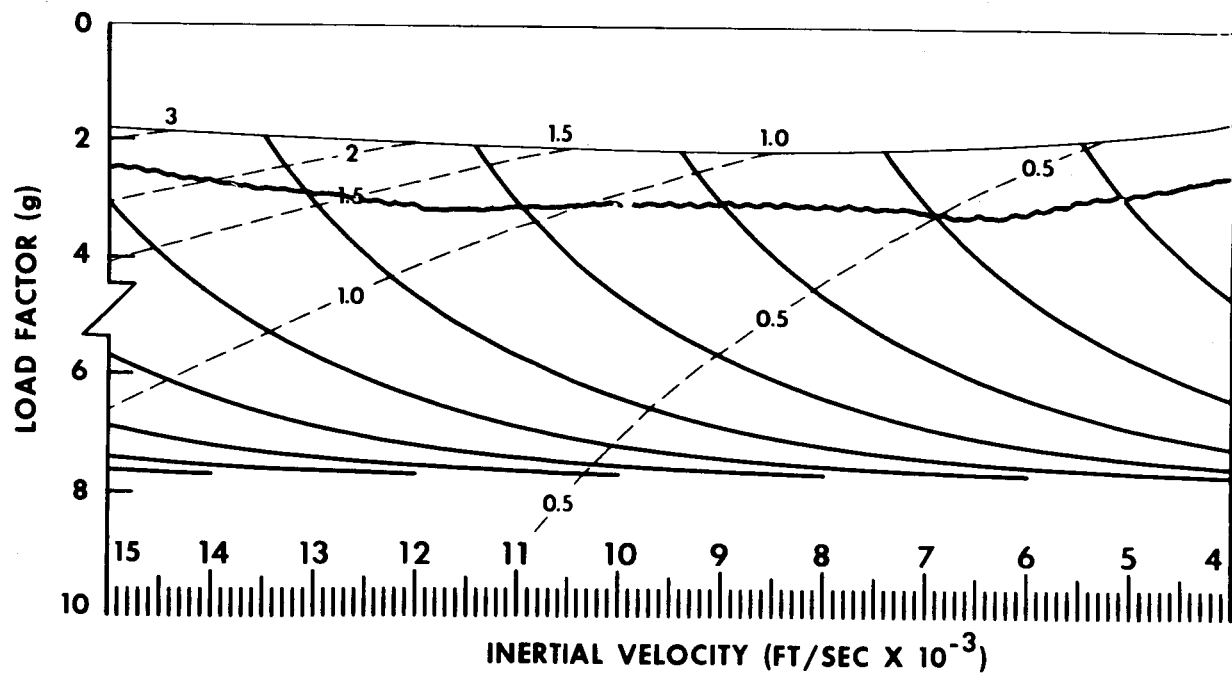
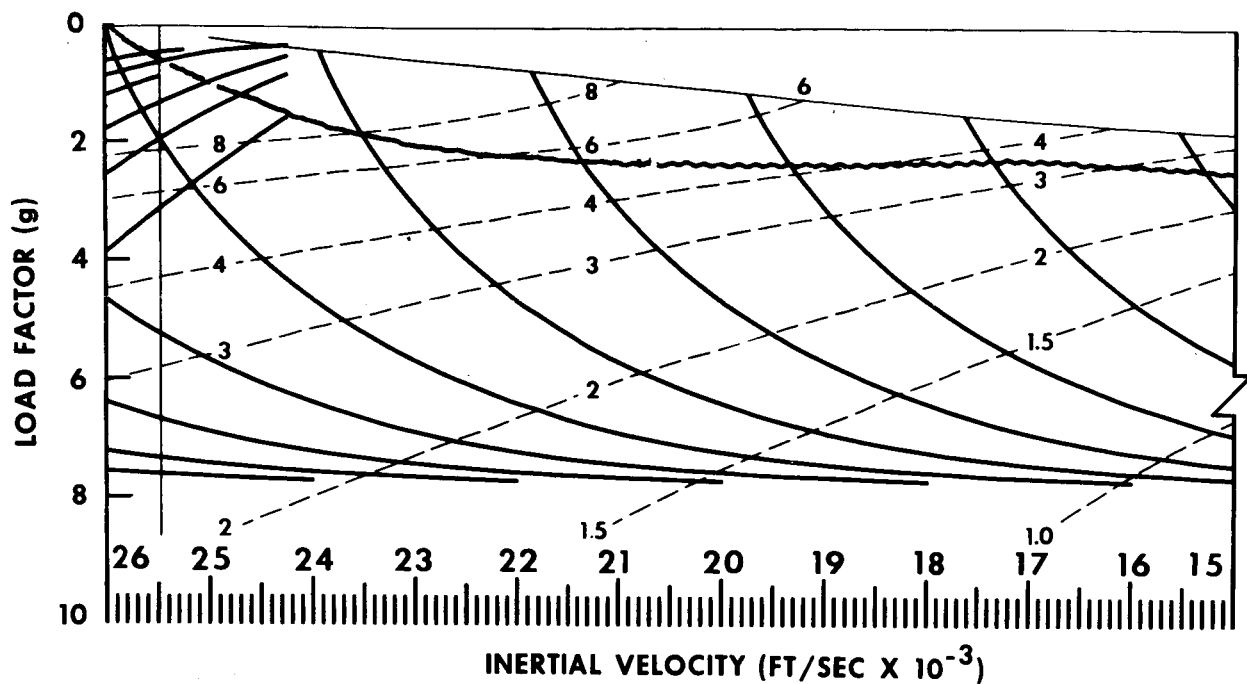


Figure 7. Apollo 7 Onboard Entry Monitor Scroll Trace

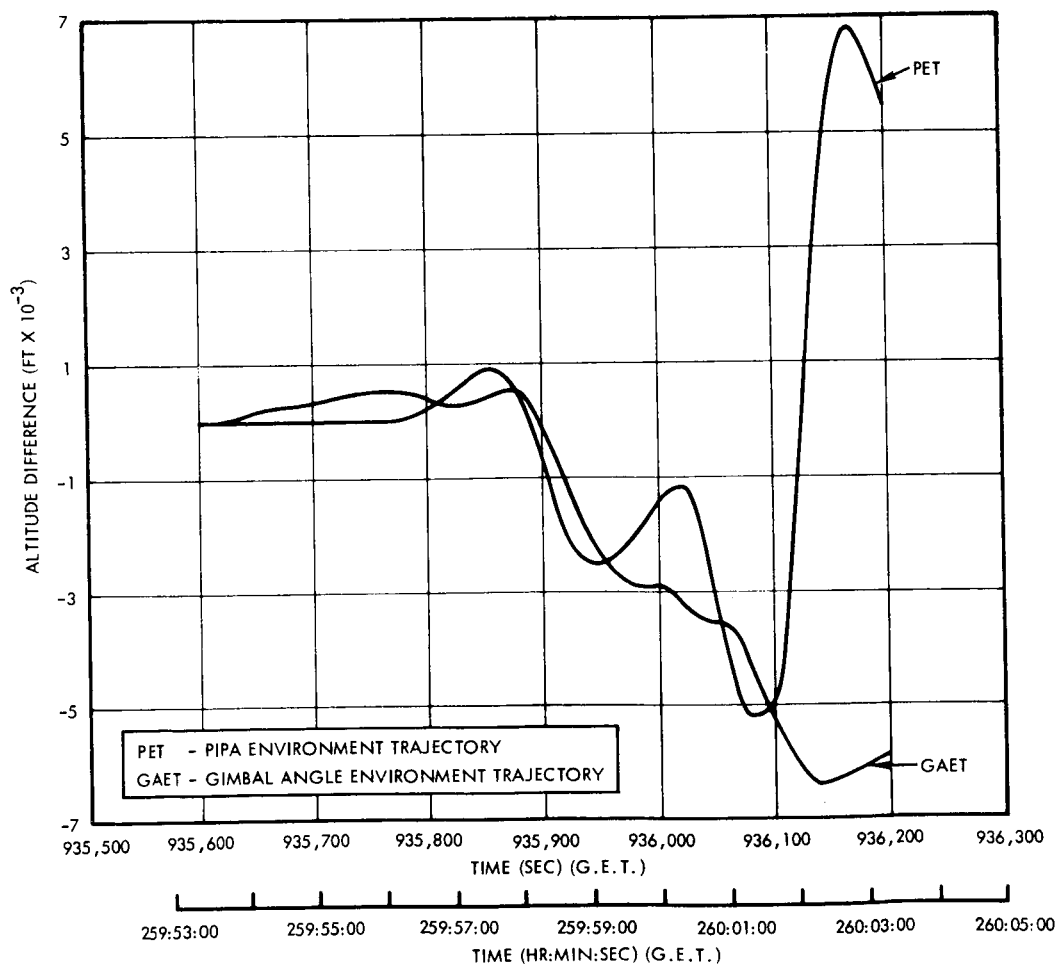
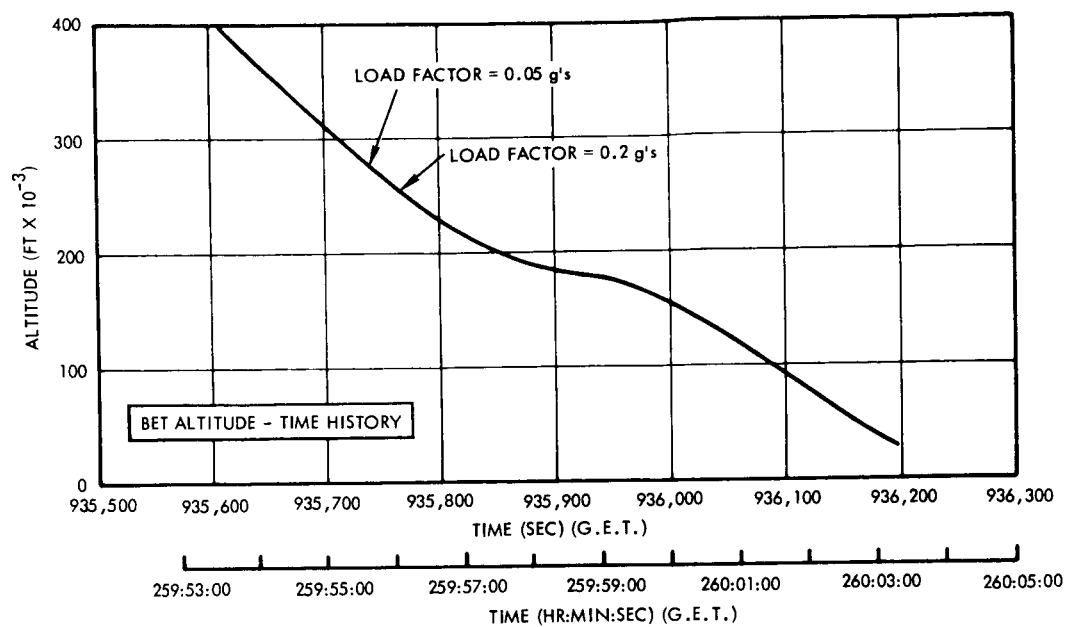


Figure 8. Altitude Time History for Apollo 7

## REFERENCES

1. Task Agreement for Reentry Mission Planning, Flight Support and Postflight Analysis for Mission C/CSM-101 and Mission D/CSM 104/LM-3. MSC/TRW Task A-190, Amendment 1, 28 October 1968.
2. Morth, R. : Entry Flight Data for Mission AS-202. MIT Report E-2031, October 1966.
3. CSM/LM Spacecraft Operational Data Book. Volume I, CSM Data Book, 1 May 1968.
4. Kamen, S. A. : Apollo 7 Postflight Mass Properties. U. S. Government Memorandum 68-FM74-527, 14 November 1968.
5. U. S. Standard Atmosphere Supplements. 1966.
6. Apollo VII Guidance, Navigation and Control System Performance Analysis - Final Report. TRW 11176-H095-R0-00, 20 December 1968.
7. Piland, R. O. : AS-205 Preliminary Meteorological Data. U. S. Government Memorandum TF4/M48-68.